Published in final edited form as:
Mol Cell. 2013 February 21; 49(4): 719–729. doi:10.1016/j.molcel.2012.12.005.

Mechanism for KRIT1 release of ICAP1-mediated integrin activation suppression

Weizhi Liu[1,*], **Kyle M. Draheim**[1,*], **Rong Zhang**[1], **David A. Calderwood**[1,2,3], and **Titus J. Boggon**[1,3,+]

[1]Department of Pharmacology, Yale University School of Medicine, 333 Cedar Street, New Haven, CT 06520

[2]Department of Cell Biology Yale University School of Medicine, 333 Cedar Street, New Haven, CT 06520

[3]Department of Yale Cancer Center, Yale University School of Medicine, 333 Cedar Street, New Haven, CT 06520

Summary

KRIT1 (Krev/Rap1 Interaction Trapped-1) mutations are observed in ~40% of autosomal dominant cerebral cavernous malformations (CCM), a disease occurring in up to 0.5% of the population. We show that KRIT1 functions as a switch for β1 integrin activation by antagonizing ICAP1 (Integrin Cytoplasmic Associated Protein-1)-mediated modulation of "inside-out" activation. We present co-crystal structures of KRIT1 with ICAP1 and ICAP1 with integrin β1 cytoplasmic tail to 2.54 Å and 3.0 Å resolution (the resolutions at which $I/\sigma I = 2$ are 2.75 Å and 3.0 Å, respectively). We find that KRIT1 binds ICAP1 by a bidentate surface, KRIT1 directly competes with integrin β1 to bind ICAP1, and that KRIT1 antagonizes ICAP1-modulated integrin activation using this site. We also find that KRIT1 contains an N-terminal Nudix domain, in a region previously designated as unstructured. We therefore provide new insights to integrin regulation and CCM-associated KRIT1 function.

Keywords

Integrin activation; crystal structure; cerebral cavernous malformation; protein-protein interaction

Introduction

Cerebral cavernous malformations (CCM) occur in up to 0.5% of the human population resulting in mulberry-shaped lesions, predominantly in the neurovasculature, that increase risk of hemorrhagic stroke (Cavalcanti et al., 2011; Revencu and Vikkula, 2006). CCM lesions are characterized by collections of irregular, dilated, thin-walled, capillary channels with a single layer of endothelium, leaky endothelial cell junctions and an altered sub-

[+]**Contact Information** To whom correspondence should be addressed: Titus J. Boggon Department of Pharmacology and the Yale Cancer Center Yale University School of Medicine, SHM B-316A 333 Cedar Street New Haven, CT 06520. Phone: 203-785-2943 Fax: 203-785-5494 titus.boggon@yale.edu.
[*]indicates equal contribution

endothelial matrix (Cavalcanti et al., 2011; Revencu and Vikkula, 2006). Familial loss-of-function mutations in *KRIT1* (*CCM1*), *CCM2*, or *PDCD10* (*CCM3*) predispose to CCM and can lead to stroke, seizures or neurological disorders (Cavalcanti et al., 2011). *KRIT1* was the first gene linked to CCM (Gunel et al., 1995) and over 40% of CCM-associated mutations occur in *KRIT1*. The disease is associated with a second acquired somatic mutation causing complete loss of KRIT1 (Akers et al., 2009; Pagenstecher et al., 2009). Recent studies of KRIT1 emphasize its role in regulation of cell-cell junctions (Stockton et al., 2010; Whitehead et al., 2009) where it acts downstream of the Rap1 GTPase (Beraud-Dufour et al., 2007; Glading et al., 2007; Liu et al., 2011), however, aberrant integrin-mediated endothelial cell adhesion to extracellular matrices is also likely to contribute to the CCM phenotype (Faurobert and Albiges-Rizo, 2010).

Integrin adhesion receptors are an evolutionally conserved family of heterodimeric glycoproteins that play essential roles during development, tissue formation, hemostasis, and in response to injury and infection (Hynes, 2002). Integrins are composed of non-covalently associated α and β subunits, each a type I trans-membrane protein with multi-domain extracellular regions, a single trans-membrane helix and a generally short cytoplasmic tail (Hynes, 2002). The cytoplasmic regions link integrins to the actin filament network and to a variety of intracellular signaling cascades (Harburger and Calderwood, 2009). Conformational changes in the extracellular domains alter integrin activation state and affinity for ligand (Kim et al., 2011a; Luo et al., 2007). These conformational changes are induced by interactions of the short integrin cytoplasmic tail with cytoplasmic proteins (Calderwood, 2004; Harburger and Calderwood, 2009; Kim et al., 2011a) an `inside-out' signaling mechanism. ICAP1 (integrin cytoplasmic-associated protein 1) is a small 200 amino acid protein that is predicted to contain a C-terminal PH/PTB fold domain that binds specifically to the integrin β1 cytoplasmic tail (Calderwood et al., 2003; Chang et al., 2002; Chang et al., 1997; Zhang and Hemler, 1999). ICAP1 is a known suppressor of integrin activation (Bouvard et al., 2007; Bouvard et al., 2003; Brunner et al., 2011) believed to act by competing with the integrin activators talin (Bouvard et al., 2007; Bouvard et al., 2003) and kindlin (Brunner et al., 2011). As ICAP1 is one of the few proteins so far shown to negatively regulate integrin activation, because it modulates focal adhesion turnover and hence matrix sensing in vitro and in vivo (Bouvard et al., 2007; Bouvard et al., 2006; Millon-Fremillon et al., 2008), and because pathways that release ICAP1-mediated suppression of integrin activation are likely to control integrin activation, understanding ICAP1's mechanism of action is highly significant.

KRIT1 is a 736 amino acid protein that contains three regions, an N-terminal NPxY motif-rich region, an ankyrin repeat domain (ARD) and a band four-point-one, ezrin, radixin, moesin (FERM) domain. The N-terminal region of KRIT1 contains three NPxY-like motifs and can bind ICAP1 (Zawistowski et al., 2002; Zhang et al., 2001). This binding competes ICAP1 from integrin cytoplasmic tails (Zhang et al., 2001) and has been suggested to sequester ICAP1 to the nucleus (Zhang et al., 2008). The discovery that mutations in KRIT1 are associated with >40% of autosomal dominant CCM (Revencu and Vikkula, 2006) highlights the clinical importance of understanding the molecular mechanisms of KRIT1 function. In the context of CCM it is notable that integrins containing the β1 subunit are required for vascular development and their loss results in altered vascular remodeling (Lei et al., 2008). β1 integrins are also important for vascular morphogenesis and essential for endothelial cell migration, adhesion and survival during angiogenesis (Abraham et al., 2008; Carlson et al., 2008; Zovein et al., 2010). This potentially implicates altered integrin adhesion dynamics in CCM, indeed ICAP1 has been implicated in formation of vascular malformations (Brutsch et al., 2011).

To probe the role of the KRIT1-ICAP1 axis as a switch that regulates integrin activation, we investigated the structural basis for KRIT1-ICAP1 and ICAP1-integrin interactions and assessed their impact on integrin activation. We determined crystal structures for the N-terminus of KRIT1 in complex with ICAP1 PTB domain and the ICAP1 PTB domain in complex with the cytoplasmic tail of integrin β1. We found that KRIT1 binds ICAP1 using a bidentate interaction surface. One part of this surface represents an unpredicted recognition motif between ICAP1 and KRIT1; the other part of this surface completely overlaps with the interaction between ICAP1 and integrin β1. Thus we provide a structural basis for KRIT1 antagonization of ICAP1-mediated suppression of integrin activation. We validate these interactions by pull-down and surface plasmon resonance assays, and show, using integrin activation assays and KRIT1 knockdown cells, that these direct binding interactions functionally impact integrin activation. Finally, we discover a previously unpredicted N-terminal Nudix domain in KRIT1.

Results

Crystal structure of KRIT1 N-terminus in complex with ICAP1 PTB domain

KRIT1 contains an N-terminal region of previously unknown structure followed by predicted ankyrin repeat and FERM domains (Fig 1A). We set out to study the interaction of the N-terminal NPxY motif-rich region with the predicted PTB domain of ICAP1 (Zawistowski et al., 2002; Zhang et al., 2001). The N-terminal portion of human KRIT1 was recalcitrant to purification but we found that co-expression with the ICAP1 PTB domain allowed co-expression and co-purification. We were thus able to determine the 2.54 Å co-crystal structure of KRIT1 residues 1 to 198 in complex with the ICAP1 PTB domain (Fig 1B and S1, **Table 1**). This provided the first atomic-level structure for these regions of KRIT1 or ICAP1 and revealed that KRIT1 residues 172–195 mediate binding to ICAP1 while the N-terminal 170 KRIT1 residues fold with high structural similarity to members of the Nudix (Nucleotide Diphosphate linked to an X moiety) group of hydrolases (Bessman et al., 1996) (discussed below).

In the KRIT1-ICAP1 co-crystal structure the ICAP1 construct spans residues 49 to 200 but the first residue visible in all copies of the asymmetric unit is $C60^{ICAP}$ and the final well-ordered residue is $Ser193^{ICAP}$. Therefore the ICAP1 PTB domain spans residues 60–193. ICAP1 adopts a Dab-like PTB/PH fold.

KRIT1 directly binds ICAP1 using an extended 24-residue region beginning at $H172^{KRIT}$ and ending at $Y195^{KRIT}$. This interface buries 2969 $Å^2$, has a shape complementarity of 0.71, and is highly conserved (Fig S2 and S3). Notably, the interaction surface is bidentate containing two distinct sites, which we term "*RR*" and "*NPxY*" (Fig 2A). *NPxY*-site residues $Ile186^{KRIT}$ to $Y195^{KRIT}$ bind ICAP1 between its β5 strand and α2 helix (Figs 1B, 2A and 2B) via a canonical PTB-NPxY binding interaction. $Y195^{KRIT}$ is clearly visible in the electron density, stacks against ICAP1 residue $I139^{ICAP}$ and hydrogen bonds to the backbone carbonyl of $Y136^{ICAP}$. In contrast, site *RR* is an unpredicted binding motif encompassing residues $H172^{KRIT}$ to $R185^{KRIT}$ (Fig 2A). The KRIT1 *RR* site wraps around the side of the ICAP1 PTB β-barrel in the form of two α-helices and is accommodated between the ICAP1 β1–β2 helix insert (helix α1) and the β5–β6 loop (Fig 1B). Interestingly the PTB insert helix α1, that is observed in Dab-like PTB domains and participates significantly in KRIT1 binding by forming one side of the *RR* site, is shifted towards the β5–β6 loop by approximately 9 Å from its location in X11 (1AQC) and other Dab-like PTB domains. The KRIT1-ICAP1 *RR* site interaction is spearheaded by two completely conserved KRIT1 arginine residues $R179^{KRIT}$ and $R185^{KRIT}$ (Fig 2A) which interact with an extensive patch of negative potential (Fig S2E) formed by $D93^{ICAP}$, $Q96^{ICAP}$ and the backbone carbonyl of $D146^{ICAP}$. The KRIT1 *RR* site forms two α-helices (α5 and α6), with

the break between them caused by the completely conserved $R179^{KRIT}$–$P180^{KRIT}$ pair, and stabilized by the completely conserved $R90^{KRIT}$ hydrogen bonding to the backbone carbonyls of $R179^{KRIT}$ and $P180^{KRIT}$ (Fig 2A). Notably, the *RR* site is a novel and unanticipated interface between KRIT1 and ICAP1 and the key ICAP1 and KRIT1 residues that mediate the interaction are completely conserved through evolution (Figs S2 and S3).

Validation of the KRIT1-ICAP1 interaction

Pull-down assays using the ICAP1-binding portion of KRIT1 (residues 170–198) confirmed that KRIT1 binds ICAP1, but revealed that point mutations in either the *RR* ($R179A^{KRIT}$/$R185A^{KRIT}$ or $A176D^{KRIT}$/$P182D^{KRIT}$) or the *NPxY* sites ($N192A^{KRIT}$/$Y195A^{KRIT}$) of KRIT1 significantly inhibited the interaction (Fig 2C and S2G). Importantly, mutating both *RR* and *NPxY* sites in tandem reduced binding to background levels (Fig 2C and S2G). Simultaneous *RR* and *NPxY* site mutations also prevented co-purification of KRIT1(1–274) with ICAP1, showing that these sites are necessary for ICAP1 binding even when the Nudix domain and all three NPxY/F motifs are present (Fig S2H). Consistent with this, ICAP1 mutations in the *NPxY*-binding site ($L135A^{ICAP}$/$I138A^{ICAP}$/$I139A^{ICAP}$ or $C184D^{ICAP}$) or at the *RR*-binding site ($I89R^{ICAP}$ or $D93A^{ICAP}$/$Q96A^{ICAP}$) significantly impaired KRIT1 binding (Fig 2D and S2I).

KRIT1 N-terminus folds as a previously unpredicted Nudix domain

In addition to the molecular basis for ICAP1-KRIT1 interactions, our structure revealed a completely unanticipated Nudix domain in KRIT1 (Fig 3A and 3B). Nudix domains are found in a diverse group of hydrolases with a wide array of substrates (e.g. nucleotide sugars, NADH, dinuceloside polyphosphates, capped RNA, nucleoside triphosphates), and are mostly, but not exclusively, characterized by the presence of a “Nudix box” motif $Gx_5Ex_7REUxEExGU$ sequence (where U is hydrophobic)(Bessman et al., 1996). KRIT1 does not include the canonical “Nudix box” motif or other Nudix motifs (Fig 3C) but does, however, very clearly adopt a Nudix fold (Fig S4) with a central β-sheet flanked by two α-helices (Bessman et al., 1996)(Fig 3B). Structural analysis revealed no indication that KRIT1 falls into any of the previously described classes of Nudix fold hydolases (Fig 3C), and superposition of KRIT1 Nudix domain on all previously determined structures of Nudix domains in complex with substrates (81 in total) does not suggest potential substrates. Consistent with our analysis, we found no evidence of KRIT1 hydrolase activity for a range of canonical nucleotide substrates (Fig 3D). While the role of the KRIT1 Nudix domain is yet to be elucidated, its presence suggests a previously unreported function for KRIT1 that must be considered in parallel to KRIT1's role in modulating cell-cell and cell-ECM adhesion.

Crystal structure of ICAP1 in complex with integrin β cytoplasmic tail

ICAP1 was first identified as an integrin β1 cytoplasmic tail-binding protein (Chang et al., 1997). Mutagenesis implicated the integrin β1 tail NPKY motif and a preceding VTTV sequence as important for ICAP1 binding, and molecular modeling suggested the interaction occurred via a classical PTB-domain ligand interaction (Chang et al., 2002), which would be expected to compete with the KRIT1-ICAP1 interaction described above. To understand the ICAP1-β1 integrin interface in detail we determined the 3.0 Å resolution co-crystal structure of ICAP1 in complex with a 15mer peptide of the integrin β1A cytoplasmic tail (residues 784 to 798) (Fig 4A, 4B and S5, **Table 1**). We found no significant conformational changes in ICAP1 between the KRIT1-bound or integrin β1-bound ICAP1 structures. The major difference is a 1–2 Å movement in the β5–β6 loop on KRIT1 binding that is probably an induced fit effect. Overall, for well-observed copies, the ICAP1-integrin β1 complex superposes with an RMSD of ~1.0 Å over ~107 Cα atoms, the ICAP1 from the integrin β1

complex superposes with an RMSD of ~1.1 Å over ~111 Cα atoms to ICAP1 from the KRIT1 complex, and the ICAP1 copies from the KRIT1-ICAP1 complex superpose with RMSD of 0.4 Å over 133 residues.

ICAP1 is bound to the β1 tail in the canonical PTB binding site between the β3 and the α5 helix allowing integrin β1 to form an antiparallel β-sheet with ICAP1 stand β3. Consistent with published mutagenic analyses (Chang et al., 2002), the interaction is mediated by integrin β1 residues $S783^{I\beta1}$ to $N792^{I\beta1}$ (SAVTTVVN). This interaction interface is highly conserved (Fig S3) and broadly hydrophobic, with $V787^{I\beta1}$ and $V790^{I\beta1}$ packing against hydrophobic patches. Direct backbone hydrogen bonds are observed between $V790^{I\beta1}$ and $N792^{I\beta1}$ of integrin β1 and $M141^{ICAP}$ and $I139^{ICAP}$ of ICAP1 forming an antiparallel β-sheet. Hydrogen bonding is also observed between the backbone and side chains of $T788^{I\beta1}$ and $C143^{ICAP}$ (Fig 4A and 4B). Surprisingly, although the β1 integrin N^{792}PxY motif binds ICAP1 and mutagenesis confirms the importance of $Y795^{I\beta1}$ (Chang et al., 2002), $Y795^{I\beta1}$ binding to the ICAP1 PTB domain is not observed in our crystal structure. In total 981 $Å^2$ are buried in the interaction between ICAP1 and integrin β1 with a shape complementarity of 0.63.

Validation of the ICAP1-integrin β1 interaction

We validated the crystallographic ICAP1-integrin β1 interaction by mutagenesis and pull-down assays (Fig 4C, 4D, S5D and S5E). We found that $T788D^{I\beta1}$/$V790D^{I\beta1}$ or $N792A^{I\beta1}$/$Y795A^{I\beta1}$ double mutations in integrin β1 very strongly inhibit ICAP1 binding, (Fig 4C and S5D). We also tested ICAP1 mutants generated for KRIT1 interaction studies and, consistent with the ICAP1-β1 crystal structure, found that *NPxY* site mutations strongly inhibited β1 tail binding while *RR* site mutations had no significant effect (Fig 4D and S5E). Thus, we show that, in contrast to the bidentate KRIT1 binding, β1 integrin binds only at the canonical PTB domain ligand-binding site, and that the interface involves β1 residues $S783^{I\beta1}$ to $N792^{I\beta1}$.

ICAP1 is a direct modulator of integrin activation

The ICAP1-binding site in the β1 tail overlaps the kindlin-binding site and abuts that for talin, two key integrin-activating proteins (Harburger and Calderwood, 2009), suggesting steric hindrance as a possible mechanism for the reported competition between ICAP1 and kindlin or talin (Bouvard et al., 2003; Brunner et al., 2011). This competition presumably explains the reported ICAP1-mediated inhibition of integrin activation (Bouvard et al., 2003). We therefore employed a well-validated flow cytometric integrin activation assay (Bouaouina et al., 2012) to examine the role of ICAP1 in integrin activation. We first showed that GFP-ICAP1 expression induced a dose-dependent inhibition of activation of chimeric αIIbα5β3β1 integrins stably expressed in CHO cells (Fig 4E). These integrins contain the cytoplasmic domains of α5β1 and so are regulated like normal β1 integrins (O'Toole et al., 1994) but have the extracellular and transmembrane domains of αIIbβ3, allowing us to assess activation by measuring binding of the ligand-mimetic anti-αIIbβ3 antibody PAC1 (Bouaouina et al., 2012). Notably, expression of comparable levels of integrin-binding defective ICAP1 mutants ($C184D^{ICAP}$ or $L135A^{ICAP}$/$I138A^{ICAP}$/$I139A^{ICAP}$) had no impact on integrin activation (Fig 4E). Cell-surface integrin expression levels (assessed in parallel with activation independent anti-integrin antibodies) were comparable in all conditions. As these experiments relied on exogenously expressed chimeric integrins we confirmed that ICAP1 also suppressed activation of endogenous CHO cell α5β1 integrins using a recombinant fragment of fibronectin as a reporter (Bouaouina et al., 2012) (Fig 4F). We then tested the effect of ICAP1 on integrin β3 activation and found that ICAP1 does not appreciably suppress activation of integrin αIIbβ3 (Fig 4G). Consistent with this, ICAP1 pulled down with β1 but not β3 integrin tails (Fig 4H). Finally, we

investigated whether ICAP1 could antagonize talin-mediated activation of β1 integrins. Cells were co-transfected with GFP or GFP-talin head and DsRed or DsRed-ICAP1 and integrin activation was assessed in cell populations with defined GFP and DsRed signals. As expected talin head enhanced integrin activation and this activation was inhibited in the presence of co-expressed ICAP1. Similar results were obtained for both endogenous and chimeric β1 integrins (Fig 4I). Thus, we establish ICAP1 as a direct inhibitor of β1 integrin activation and an antagonist of talin-mediated β1 integrin activation, and show that ICAP1-mediated modulation of β1 integrin activation requires formation of a typical PTB-peptide β-sheet between integrin β1 and ICAP1.

Detailed comparison of integrin β 1 and KRIT1 binding to ICAP1

Analysis of the modes of binding of KRIT1 and integrin β1 to ICAP1 reveals similarities and differences. For KRIT1 the NPxY tyrosine, $Y195^{KRIT}$, which is at the C-terminus of a short 3_{10} helix encompassing the $P193^{KRIT}$, $A194^{KRIT}$ and $Y195^{KRIT}$, packs against a hydrophobic patch at the N-terminus of β5 formed by $I139^{ICAP}$ and hydrogen bonds to the backbone carbonyl of $Y136^{ICAP}$. For integrin β1 $Y795^{Iβ1}$ is only visible in the electron density for one built copy, where it is extended away from ICAP1. $Y795^{Iβ1}$ is known to be important for binding ICAP1 (Chang et al., 2002), and our pull-down assays confirm a role for this residue (Fig 4C, 4H), but it is poorly ordered in our crystal structure and is apparently not intrinsic to the interaction (Fig S5C). It is not clear from the structure why the integrin β1 peptide (which includes residues to the extreme C-terminus of integrin β1) does not form a 3_{10} helix or type I β-turn on binding to ICAP1, there are no crystal contacts that would perturb this binding, and solvent channels are nearby that allow C-terminal residues to be accommodated.

N-terminal to the NPxY motif, both integrin β1 and KRIT1 form an extended anti-parallel β-sheet with ICAP1 strand β5 spanning residues $V787^{Iβ1}$-$V791^{Iβ1}$ (sequence: VTTVV) in integrin β1 and $K187^{KRIT}$-$I191^{KRIT}$ (sequence: KTNVI) in KRIT1 (Fig 5A). A similar hydrophobic/hydrogen-bonding profile is found for both integrin β1 and KRIT1 binding. This is typified by $V790^{Iβ1}$ and $V190^{KRIT1}$ which pack snugly in an experimentally identical fashion into an hydrophobic pocket formed by $L187^{ICAP}$, $S188^{ICAP}$, $M141^{ICAP}$ and $C184^{ICAP}$. Interestingly, while ICAP1 is specific for integrin β1 over β3 (Chang et al., 1997)(Fig 4H), the structure does not provide a clear explanation for the mechanism of specificity.

To measure the affinity of the interactions of ICAP1 with integrin β1 and KRIT1 we conducted surface plasmon resonance (SPR) (Fig S6A). We found a K_D of 1.24 ± 0.03 μM for the ICAP1-KRIT1 interaction and K_D of 5.0 ± 0.15 μM for the ICAP1-integrin β1, approximately a 4-fold increase in affinity between ICAP1 and KRIT1 compared to ICAP1 and integrin β1 (Fig S6A). Additionally, our SPR measurements qualitatively suggest that the dissociation of ICAP1 from KRIT1 is slower than the dissociation of ICAP1 from integrin β1. These data correlate well with our structural data.

KRIT1 antagonizes ICAP1 modulation of integrin activation

The *NPxY* site of ICAP1 is used to bind either integrin β1 or KRIT1. Superposition of ICAP1-KRIT1 and ICAP1-β1 structures reveals the similarities between these interactions (Fig 5A) and suggests that KRIT1 and β1 integrin will compete for ICAP1 binding. To confirm this we used purified recombinant proteins to show that GST-KRIT1(170–198) and GST-β1 tails compete for binding to His-ICAP1(49–200) coated beads (Fig 5B). Furthermore, competition was reduced using an ICAP1-binding-deficient KRIT1 mutant (Fig 5B). This, together with our data showing ICAP1 suppresses integrin activation (Fig 4D), suggests that KRIT1 will antagonize the inhibitory effect of ICAP1 on β1 integrin

activation via direct competition at the ICAP1 *NPxY* site. To test this we assessed the effect of co-expressed GFP-tagged KRIT1 on DsRed-ICAP1-mediated suppression of β1 integrin activation in CHO cells. β1 integrin activation was measured in double GFP- DsRed-positive populations by flow cytometry (Fig S6B and S6C). Whereas co-expression of GFP and DsRed-ICAP1 represses activation of chimeric or endogenous β1 integrins, co-expression of GFP-KRIT1(1–198) with DsRed-ICAP1 restores integrin activation (Fig 5C and 5D), presumably by sequestering ICAP1 away from integrins. Consistent with this idea, ICAP1-binding defective KRIT1 mutants fail to antagonize ICAP1 repression of integrin activation (Fig 5C). Interestingly, a shorter KRIT1 construct (170–198), which lacks the Nudix domain only partially restores integrin activation indicating a potential contribution of the Nudix domain (Fig 5C). KRIT1 therefore antagonizes ICAP1 modulation of integrin activation by direct competition with the integrin binding site.

Loss of KRIT1 decreases integrin activation

Finally, to further test our hypothesis that KRIT1 antagonizes ICAP1-mediated integrin suppression we investigated the consequences of KRIT1 knockdown in two more physiologically relevant human cell types, EA.hy926 endothelial cells and U118 glioblastoma cells, that each express endogenous KRIT1 and ICAP1 (Fig 5E). Cells were infected with lentiviral constructs encoding one of two separate shRNAs targeting human KRIT1 (shKRIT1-1 and shKRIT1-2) or a control shRNA against luciferase. Infected cells were selected based on puromycin resistance and GFP expression and integrin activation was assessed by flow cytometry in GFP positive cells. Both shRNA constructs targeting KRIT1 reduced endogenous KRIT1 expression in EA.hy926 and U118 cells (Fig 5E), and also significantly inhibited activation of endogenous α5β1 in both cell types, when compared with uninfected parental cells or cells infected with control luciferase shRNA (Fig 5F). Notably, the effect on activation was strongest for the shKRIT1-2 construct which produces the greatest KRIT1 knockdown (Fig 5F). These data clearly implicate KRIT1 in regulation of integrin activation.

To further substantiate our model where KRIT1 binding to ICAP1 prevents ICAP1-mediated inhibition of integrin activation we performed rescue experiments in KRIT1 knockdown U118 cells with a KRIT1 fragment not targeted by shKRIT1-1 or shKRIT1-2. Expression of the DsRed-tagged ICAP1-binding fragment of KRIT1(1–198) in KRIT1-knockdown U118 cells reversed the observed inhibition of integrin activation but this reversal was not evident when KRIT1 mutants defective in ICAP1 binding were used (Fig 5G). Taken together with our structural and biochemical studies these data confirm that KRIT1-ICAP1 interactions are important for KRIT1-mediated regulation of integrin activation and support a model where competition between KRIT1 and integrin for binding to ICAP1 modulates integrin activation (Fig 6).

Discussion

Integrin activation is tightly regulated through association of activating or inhibitory proteins with the integrin cytoplasmic tails (Kim et al., 2011a). This in turn influences a wide range of cellular phenotypes including cell adhesion, migration, signaling and differentiation and so controls key physiological and pathological processes. While the process of integrin activation is increasingly well understood (Harburger and Calderwood, 2009), relatively few direct inhibitors of activation have been identified. ICAP1 is one of the better-characterized inhibitors in integrin activation (Faurobert and Albiges-Rizo, 2010; Kim et al., 2011a). ICAP1 selectively binds integrin β1 cytoplasmic tails and is believed to suppress activation by preventing the binding of integrin activators talin and kindlin (Bouvard et al., 2007; Bouvard et al., 2003; Brunner et al., 2011). Stimulated integrin activation may therefore require mechanisms to release ICAP1-mediated suppression. Here we have used X-ray

crystallography, protein biochemistry, and cell-based integrin activation assays to characterize ICAP1-β1 integrin interactions, to show that ICAP1-integrin interactions are required to suppress integrin activation, and to reveal that KRIT1 competes with integrin β tails for binding to ICAP1 and hence that KRIT1 antagonizes ICAP1-mediated suppression of β1 integrin activation. Notably, loss of function mutations in KRIT1 are observed in ~40% of familial cerebral cavernous malformations (CCM), a disease occurring in up to 0.5% of the population (Cavalcanti et al., 2011; Revencu and Vikkula, 2006). Our data suggest that loss of KRIT1 in CCM may lead to reduced β1 activation, potentially contributing to the leaky vasculature (Faurobert and Albiges-Rizo, 2010; Lei et al., 2008). Indeed our knockdown studies confirm that loss of KRIT1 impairs α5β1 activation in two independent cell types. Whether integrin activation is similarly inhibited in CCM lesions in vivo remains to be determined; one study suggests that ICAP1 may also be lost from KRIT1-deficient lesions (Zhang et al., 2008) potentially increasing β1 integrin activation in CCM. Nonetheless, we did not observe loss of ICAP1 from KRIT1 knockdown cells and our data strongly suggest that integrin signaling may be altered in CCM. In addition, our structures reveal that KRIT1 contains an N-terminal Nudix domain in a region previously designated as unstructured. These studies therefore provide insight to the understanding of both integrin regulation and CCM disease.

Implications for understanding ICAP1 action as a suppressor of integrin activation

ICAP1 was first identified as an integrin β1 tail-binding protein (Chang et al., 1997) and was subsequently shown to regulate β1 integrin-mediated cell spreading, cell migration and focal adhesion dynamics (Bouvard et al., 2003). ICAP1 competes with the integrin activating protein talin for binding to integrin β1 tails in vitro (Bouvard et al., 2003), ICAP1 over-expression inhibits kindlin-2 binding to β1 tails (Brunner et al., 2011), and ICAP1-deficient mice have osteoblast defects consistent with increased integrin activation (Bouvard et al., 2007). Together these data suggest that ICAP1 functions as a direct suppressor of integrin activation through competition with talin and kindlin (Bouvard et al., 2007; Bouvard et al., 2003; Brunner et al., 2011). The ICAP1 binding site on integrin β1 revealed by this study is immediately adjacent to the structurally-defined talin-integrin interaction site (Anthis et al., 2009) and overlaps with the kindlin-binding site on integrin β1 tails defined by mutagenesis (Harburger et al., 2009), raising the potential of steric hindrance or direct competition. Our functional studies establish that ICAP1 suppresses β1 integrin activation and that direct ICAP1-β1 interactions are required for this suppression.

Mechanism for KRIT1 release of ICAP1-mediated integrin activation suppression

KRIT1 function is still being deciphered. It has been shown to interact with microtubules (Gunel et al., 2002) and is released from microtubules by Rap1 small GTPase binding to the FERM domain (Beraud-Dufour et al., 2007; Liu et al., 2011). Rap1 also enhances KRIT1 localization to cell-cell contacts, perhaps through interactions with heart-of-glass receptor and β-catenin (Kleaveland et al., 2009; Liu et al., 2011). KRIT1 also interacts with ICAP1 and as shown here, this releases ICAP1 from integrin β tails, potentially facilitating nuclear translocation of ICAP1 (Faurobert and Albiges-Rizo, 2010; Fournier et al., 2005) and preventing further competition with talin and kindlin. Phosphorylation of ICAP1 by CamKII is one mechanism that has been suggested to impact binding specificity to integrin β1 or KRIT1 (Bouvard et al., 2006; Kim et al., 2011b). Our structural, biochemical and functional data support a KRIT1-specific release mechanism for ICAP1 suppression of integrin activation (Fig 6). As both KRIT1 and ICAP1 contain nuclear localization signals, there is the potential that the KRIT1-ICAP1 complex can then be efficiently targeted away from the membrane to allow talin or kindlin-mediated integrin activation.

The KRIT1 Nudix domain

The discovery of the Nudix domain in KRIT1 is surprising. No previous prediction suggested that the KRIT1 N-terminus contains any folded region and on comparison of the KRIT1 Nudix domain with structures of Nudix fold proteins, the structure-based sequence identity is on average only 11%. The role of the KRIT1 Nudix domain is unclear. These enzymes have extremely diverse substrates, so if KRIT1 Nudix is a functional enzyme the discovery of its substrate may be non-trivial. Furthermore, Nudix domains can also play roles as protein or DNA-interaction partners, raising the possibility that the KRIT1 Nudix domain could interact with diverse partners at microtubules, the cell membrane, or in the nucleus. Elucidation of the proper function of the KRIT1 Nudix domain may provide an important step to understanding the roles of KRIT1 in normal tissues and in CCM disease.

Implications for understanding KRIT1 function and CCM disease

In addition to their importance for the understanding of normal integrin signaling, as ~40% of CCM cases are associated with loss of KRIT1 our findings will improve understanding of the pathology and etiology of this life-threatening disorder. Recent studies have focused on the roles of KRIT1 in Rho/ROCK and Rap1 signaling pathways (Liu et al., 2011; McDonald et al., 2010). Our findings suggest that loss of KRIT1 should also reduce β1 activation, potentially contributing to a leaky vasculature (Faurobert and Albiges-Rizo, 2010; Lei et al., 2008). Finally, our discovery of an unexpected N-terminal Nudix domain in KRIT1 reveals the potential for KRIT1 enzymatic activity and highlights the need to identify KRIT1 substrates and to test their roles in the pathology and etiology of CCM.

Experimental Procedures

Full methods are provided in the Supplemental Experimental Procedures.

ICAP1 expression and purification

Codon-optimized human ICAP1 (residues 49–200) was expressed as a GST-fusion protein and was purified to homogeneity by anion exchange and size exclusion chromatography. Selenomethionine-labeled ICAP1 was purified as per the native protein.

ICAP1-integrin β1 co-crystallization

Before crystallization trials, ICAP1 was concentrated to 5.0 mg/ml and incubated with a peptide from the C-terminal tail of integrin β1 (K^{784}SAVTTVVNPKYEGK) in a 1:2 ratio (protein:peptide). Crystals grew in precipitant conditions of 1.15 – 1.25 M sodium citrate, pH 6.5. The final refined structure of ICAP1 in complex with integrin β1 is for a SeMet substituted protein crystal.

KRIT1-ICAP1 co-expression and co-purification

The N-terminal portion of KRIT1 was recalcitrant to purification on its own. Therefore we conducted a co-expression and co-purification protocol for the KRIT1-ICAP1 complex using human KRIT1 (residues 1 – 198) and codon-optimized human ICAP1 (residues 49–200).

KRIT1-ICAP1 co-crystallization

KRIT1-ICAP1 complex was concentrated to ~20.0 mg/ml for crystallization. The best crystals grew within 4 to 7 days at room temperature by hanging drop vapor diffusion using precipitant conditions of 2.04 to 2.08 M $AmSO_4$, 0.2 M ammonium formate. For

cryoprotection, the crystals were transferred to 3.2 M $AmSO_4$ substituted with 0.5 M NaBr and then flash frozen in liquid nitrogen prior to data collection.

Structure determination and refinement

The 3.0 Å structure of selenomethionine substituted ICAP1-integrin β1 complex was determined using SAD phasing. This allowed a model to be generated that could be used for molecular replacement for the 2.54Å KRIT1-ICAP1 structure. The molecular replacement solution provided a seed for automated model building which accurately built almost the whole structure of ICAP1 in the KRIT1-ICAP1 complex; manual building and refinement completed the structure of KRIT1-ICAP1. This completed model of refined ICAP1 was then used as a molecular replacement model for the ICAP1-integrin β1 complex and standard refinement and model building completed the structure.

Generation of ICAP1 mutant proteins and pull-down assays

GST-integrin β1 fusion protein (residues 752 to 798) or GST-KRIT1 (residues 170 to 198) were bound to beads and incubated with His-tagged ICAP1. Pull-down assays were all conducted more than three times and showed consistent results. ICAP1 mutants were generated by site-directed mutagenesis.

Competition assay

GST-integrin β1 and His-ICAP1 were purified and mixed with Nickel resin (Novagen) in the presence of increasing amounts of GST-KRIT1(170–198). The relative amount GST-integrin β1 remaining bound to nickel beads was measured.

KRIT1-N-terminal Nudix-like domain enzymatic assay

The enzymatic activity of N-terminal KRIT1 Nudix domain was examined by measuring release free phosphate using the Malachite green reagents (BioAssay Systems). Then the absorption of 620 nm was measured using a SAFIRE plate reader (Tecan), this was compared to measurements for no enzyme and the difference plotted in Fig 3D. Each measurement was repeated at least three times.

Cell culture and integrin activation assays

A previously described CHO cell line stably expressing chimeric αIIbα5β3β1 integrins (O'Toole et al., 1994) was used for all integrin activation assays and integrin activation states were assessed in three-color FACS assays using a modification of previously described methods (Bouaouina et al., 2012).

Surface Plasmon Resonance

GST, GST-KRIT1 (residues 170–198), GST-KRIT1-mut ($R179A^{KRIT}$/$R185A^{KRIT}$/$N192A^{KRIT}$/$Y195A^{KRIT}$ quadruple mutation) and GST-integrin β1 were used as ligand and ICAP1 as the analyte. Binding assays were performed using a Biacore T100 (GE).

shRNA

Lentiviral shRNA constructs were from Open Biosystems. Lentiviruses were produced by cotransfecting packaging vectors psPAX2 and pMD2.G (Addgene) into HEK-293T cells with the shRNA construct. Viral supernatant was collected, filtered, and incubated with target cells. Infected cells were selected with 2 μg/mL Puromycin. Re-expression of KRIT1 was achieved by nucleofection (AMAXA).

Supplementary Material

Refer to Web version on PubMed Central for supplementary material.

Acknowledgments

We thank V. Stojanoff, J. Jakoncic, X. Li, A. Stiegler, N. Alicea-Velazquez, J. Hu, W. Min, K. Reinisch, E. Folta-Stogniew, B. Turk, S-E. Jordt, A. Koleske, Y. Ha and beamlines X25, X6A and X29 (NSLS) NECAT (APS). TJB and DAC are funded by the NIH. KMD is a recipient of an American Cancer Society postdoctoral fellowship.

References

Abraham S, Kogata N, Fassler R, Adams RH. Integrin β1 subunit controls mural cell adhesion, spreading, and blood vessel wall stability. Circ Res. 2008; 102:562–570. [PubMed: 18202311]

Akers AL, Johnson E, Steinberg GK, Zabramski JM, Marchuk DA. Biallelic somatic and germline mutations in cerebral cavernous malformations (CCMs): evidence for a two-hit mechanism of CCM pathogenesis. Hum Mol Genet. 2009; 18:919–930. [PubMed: 19088123]

Anthis NJ, Wegener KL, Ye F, Kim C, Goult BT, Lowe ED, Vakonakis I, Bate N, Critchley DR, Ginsberg MH, Campbell ID. The structure of an integrin/talin complex reveals the basis of inside-out signal transduction. Embo J. 2009; 28:3623–3632. [PubMed: 19798053]

Beraud-Dufour S, Gautier R, Albiges-Rizo C, Chardin P, Faurobert E. Krit 1 interactions with microtubules and membranes are regulated by Rap1 and integrin cytoplasmic domain associated protein-1. Febs J. 2007; 274:5518–5532. [PubMed: 17916086]

Bessman MJ, Frick DN, O'Handley SF. The MutT proteins or “Nudix” hydrolases, a family of versatile, widely distributed, “housecleaning” enzymes. J Biol Chem. 1996; 271:25059–25062. [PubMed: 8810257]

Bouaouina M, Harburger DS, Calderwood DA. Talin and signaling through integrins. Methods Mol Biol. 2012; 757:325–347. [PubMed: 21909921]

Bouvard D, Aszodi A, Kostka G, Block MR, Albiges-Rizo C, Fassler R. Defective osteoblast function in ICAP-1-deficient mice. Development. 2007; 134:2615–2625. [PubMed: 17567669]

Bouvard D, Millon-Fremillon A, Dupe-Manet S, Block MR, Albiges-Rizo C. Unraveling ICAP-1 function: toward a new direction? Eur J Cell Biol. 2006; 85:275–282. [PubMed: 16546571]

Bouvard D, Vignoud L, Dupe-Manet S, Abed N, Fournier HN, Vincent-Monegat C, Retta SF, Fassler R, Block MR. Disruption of focal adhesions by integrin cytoplasmic domain-associated protein-1 alpha. J Biol Chem. 2003; 278:6567–6574. [PubMed: 12473654]

Brunner M, Millon-Fremillon A, Chevalier G, Nakchbandi IA, Mosher D, Block MR, Albiges-Rizo C, Bouvard D. Osteoblast mineralization requires β1 integrin/ICAP-1-dependent fibronectin deposition. J Cell Biol. 2011; 194:307–322. [PubMed: 21768292]

Brutsch R, Liebler SS, Wustehube J, Bartol A, Herberich SE, Adam MG, Telzerow A, Augustin HG, Fischer A. Integrin cytoplasmic domain-associated protein-1 attenuates sprouting angiogenesis. Circ Res. 2011; 107:592–601. [PubMed: 20616313]

Calderwood DA. Integrin activation. J Cell Sci. 2004; 117:657–666. [PubMed: 14754902]

Calderwood DA, Fujioka Y, de Pereda JM, Garcia-Alvarez B, Nakamoto T, Margolis B, McGlade CJ, Liddington RC, Ginsberg MH. Integrin β cytoplasmic domain interactions with phosphotyrosine-binding domains: a structural prototype for diversity in integrin signaling. Proc Natl Acad Sci U S A. 2003; 100:2272–2277. [PubMed: 12606711]

Carlson TR, Hu H, Braren R, Kim YH, Wang RA. Cell-autonomous requirement for β1 integrin in endothelial cell adhesion, migration and survival during angiogenesis in mice. Development. 2008; 135:2193–2202. [PubMed: 18480158]

Cavalcanti DD, Kalani MY, Martirosyan NL, Eales J, Spetzler RF, Preul MC. Cerebral cavernous malformations: from genes to proteins to disease. J Neurosurg. 2011; 116:122–132. [PubMed: 21962164]

Chang DD, Hoang BQ, Liu J, Springer TA. Molecular basis for interaction between Icap1 alpha PTB domain and β1 integrin. J Biol Chem. 2002; 277:8140–8145. [PubMed: 11741908]

Chang DD, Wong C, Smith H, Liu J. ICAP-1, a novel β1 integrin cytoplasmic domain-associated protein, binds to a conserved and functionally important NPXY sequence motif of β1 integrin. J Cell Biol. 1997; 138:1149–1157. [PubMed: 9281591]

Faurobert E, Albiges-Rizo C. Recent insights into cerebral cavernous malformations: a complex jigsaw puzzle under construction. Febs J. 2010; 277:1084–1096. [PubMed: 20096036]

Fournier HN, Dupe-Manet S, Bouvard D, Luton F, Degani S, Block MR, Retta SF, Albiges-Rizo C. Nuclear translocation of integrin cytoplasmic domain-associated protein 1 stimulates cellular proliferation. Mol Biol Cell. 2005; 16:1859–1871. [PubMed: 15703214]

Glading A, Han J, Stockton RA, Ginsberg MH. KRIT-1/CCM1 is a Rap1 effector that regulates endothelial cell cell junctions. J Cell Biol. 2007; 179:247–254. [PubMed: 17954608]

Gunel M, Awad IA, Anson J, Lifton RP. Mapping a gene causing cerebral cavernous malformation to 7q11.2-q21. Proc Natl Acad Sci U S A. 1995; 92:6620–6624. [PubMed: 7604043]

Gunel M, Laurans MS, Shin D, DiLuna ML, Voorhees J, Choate K, Nelson-Williams C, Lifton RP. KRIT1, a gene mutated in cerebral cavernous malformation, encodes a microtubule-associated protein. Proc Natl Acad Sci U S A. 2002; 99:10677–10682. [PubMed: 12140362]

Harburger DS, Bouaouina M, Calderwood DA. Kindlin-1 and -2 directly bind the C-terminal region of β integrin cytoplasmic tails and exert integrin-specific activation effects. J Biol Chem. 2009; 284:11485–11497. [PubMed: 19240021]

Harburger DS, Calderwood DA. Integrin signalling at a glance. J Cell Sci. 2009; 122:159–163. [PubMed: 19118207]

Hynes RO. Integrins: bidirectional, allosteric signaling machines. Cell. 2002; 110:673–687. [PubMed: 12297042]

Kim C, Ye F, Ginsberg MH. Regulation of integrin activation. Annu Rev Cell Dev Biol. 2011a; 27:321–345. [PubMed: 21663444]

Kim J, Sherman NE, Fox JW, Ginsberg MH. Phosphorylation sites in the cerebral cavernous malformations complex. J Cell Sci. 2011; 124:3929–3932. [PubMed: 22194303]

Kleaveland B, Zheng X, Liu JJ, Blum Y, Tung JJ, Zou Z, Sweeney SM, Chen M, Guo L, Lu MM, et al. Regulation of cardiovascular development and integrity by the heart of glass-cerebral cavernous malformation protein pathway. Nat Med. 2009; 15:169–176. [PubMed: 19151727]

Lei L, Liu D, Huang Y, Jovin I, Shai SY, Kyriakides T, Ross RS, Giordano FJ. Endothelial expression of β1 integrin is required for embryonic vascular patterning and postnatal vascular remodeling. Mol Cell Biol. 2008; 28:794–802. [PubMed: 17984225]

Liu JJ, Stockton RA, Gingras AR, Ablooglu AJ, Han J, Bobkov AA, Ginsberg MH. A Mechanism of Rap1-Induced Stabilization of Endothelial Cell-Cell Junctions. Mol Biol Cell. 2011; 22:2509–2519. [PubMed: 21633110]

Luo BH, Carman CV, Springer TA. Structural basis of integrin regulation and signaling. Annu Rev Immunol. 2007; 25:619–647. [PubMed: 17201681]

McDonald DA, Shenkar R, Shi C, Stockton RA, Akers AL, Kucherlapati MH, Kucherlapati R, Brainer J, Ginsberg MH, Awad IA, Marchuk DA. A novel mouse model of cerebral cavernous malformations based on the two-hit mutation hypothesis recapitulates the human disease. Hum Mol Genet. 2010; 20:211–222. [PubMed: 20940147]

Millon-Fremillon A, Bouvard D, Grichine A, Manet-Dupe S, Block MR, Albiges-Rizo C. Cell adaptive response to extracellular matrix density is controlled by ICAP-1-dependent β1-integrin affinity. J Cell Biol. 2008; 180:427–441. [PubMed: 18227284]

Nakamura T, Meshitsuka S, Kitagawa S, Abe N, Yamada J, Ishino T, Nakano H, Tsuzuki T, Doi T, Kobayashi Y, et al. Structural and dynamic features of the MutT protein in the recognition of nucleotides with the mutagenic 8-oxoguanine base. J Biol Chem. 2010; 285:444–452. [PubMed: 19864691]

O'Toole TE, Katagiri Y, Faull RJ, Peter K, Tamura R, Quaranta V, Loftus JC, Shattil SJ, Ginsberg MH. Integrin cytoplasmic domains mediate inside-out signal transduction. J Cell Biol. 1994; 124:1047–1059. [PubMed: 7510712]

Pagenstecher A, Stahl S, Sure U, Felbor U. A two-hit mechanism causes cerebral cavernous malformations: complete inactivation of CCM1, CCM2 or CCM3 in affected endothelial cells. Hum Mol Genet. 2009; 18:911–918. [PubMed: 19088124]

Revencu N, Vikkula M. Cerebral cavernous malformation: new molecular and clinical insights. J Med Genet. 2006; 43:716–721. [PubMed: 16571644]

Stockton RA, Shenkar R, Awad IA, Ginsberg MH. Cerebral cavernous malformations proteins inhibit Rho kinase to stabilize vascular integrity. J Exp Med. 2010; 207:881–896. [PubMed: 20308363]

Whitehead KJ, Chan AC, Navankasattusas S, Koh W, London NR, Ling J, Mayo AH, Drakos SG, Jones CA, Zhu W, et al. The cerebral cavernous malformation signaling pathway promotes vascular integrity via Rho GTPases. Nat Med. 2009; 15:177–184. [PubMed: 19151728]

Zawistowski JS, Serebriiskii IG, Lee MF, Golemis EA, Marchuk DA. KRIT1 association with the integrin-binding protein ICAP-1: a new direction in the elucidation of cerebral cavernous malformations (CCM1) pathogenesis. Hum Mol Genet. 2002; 11:389–396. [PubMed: 11854171]

Zhang J, Basu S, Rigamonti D, Dietz HC, Clatterbuck RE. Krit1 modulates β1-integrin-mediated endothelial cell proliferation. Neurosurgery. 2008; 63:571–578. discussion 578. [PubMed: 18812969]

Zhang J, Clatterbuck RE, Rigamonti D, Chang DD, Dietz HC. Interaction between krit1 and icap1alpha infers perturbation of integrin β1-mediated angiogenesis in the pathogenesis of cerebral cavernous malformation. Hum Mol Genet. 2001; 10:2953–2960. [PubMed: 11741838]

Zhang XA, Hemler ME. Interaction of the integrin β1 cytoplasmic domain with ICAP-1 protein. J Biol Chem. 1999; 274:11–19. [PubMed: 9867804]

Zovein AC, Luque A, Turlo KA, Hofmann JJ, Yee KM, Becker MS, Fassler R, Mellman I, Lane TF, Iruela-Arispe ML. β1 integrin establishes endothelial cell polarity and arteriolar lumen formation via a Par3-dependent mechanism. Dev Cell. 2010; 18:39–51. [PubMed: 20152176]

Highlights

- Co-crystal structure of KRIT1 with ICAP1 shows a bidentate interaction interface
- Co-crystal structure of ICAP1 with integrin β1 shows a PTB-peptide interaction
- KRIT1 antagonizes ICAP1-modulated integrin activation by the bidentate interaction
- KRIT1 contains a previously undescribed N-terminal Nudix domain

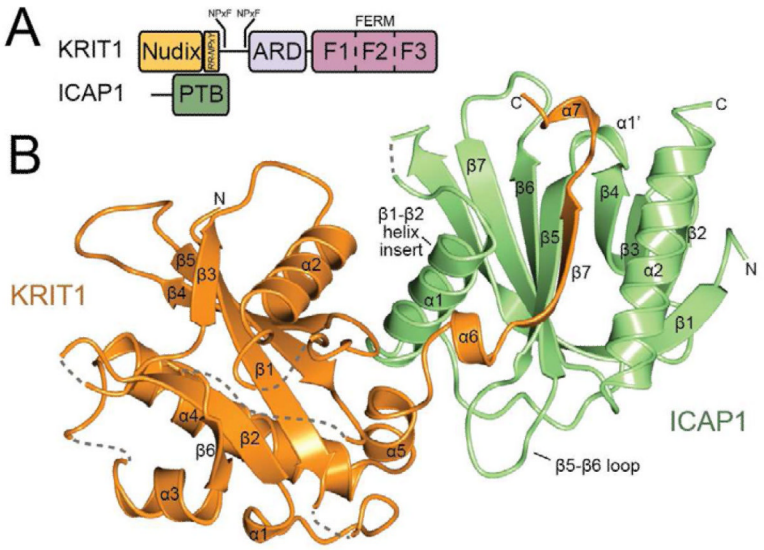

Fig. 1. Structural basis for the KRIT1-ICAP1 complex

A) Domain schematic of KRIT1. This study reveals that KRIT1 contains an N-terminal Nudix domain followed by the bidentate ICAP1-binding region; sites *RR* and *NPxY*. C-terminal to this there are two NPxF motifs, an ankyrin repeat domain (ARD) and a FERM domain that includes sub-domains F1, F2 and F3. **B)** Overall structure of KRIT1 in complex with ICAP1. ICAP1 is shown in green and KRIT1 in salmon. Dashed lines indicate unstructured loops. See also Figure S1.

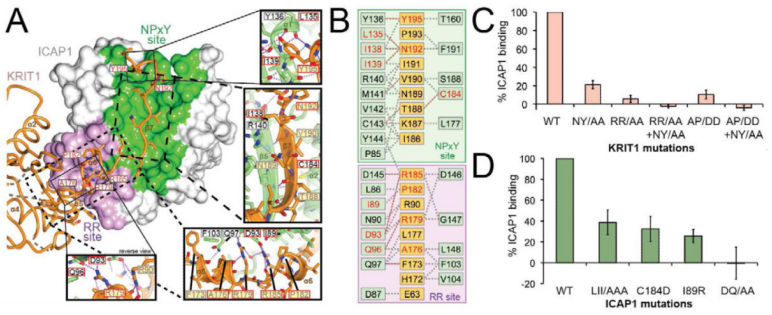

Fig. 2. KRIT1 binds ICAP1 using a bidentate interaction surface

A) KRIT1-ICAP1 co-crystal structure with the surface of ICAP1 shown. KRIT1 (in salmon) directly binds both the "*NPxY*" site of ICAP1 shown in green, and the "*RR*" site shown in purple. Exploded views show the mode of KRIT1 binding to the *NPxY* and *RR* sites. Residues mutated in this study are indicated in red. **B)** Schematic map showing the interactions between KRIT1 (orange) and ICAP1 (green). Mutated residues are colored red and both the RR and NPxY sites are indicated. Hydrogen bonds indicated by red lines and non-bonding contacts as dashed lines. **C** and **D)** Pull-down assays demonstrate that mutations in either the *RR* or *NPxY* interfaces inhibit ICAP1$^{49–200}$ binding to KRIT1$^{170–198}$, but that mutation in both sites reduces binding to undetectable levels. Densitometry was used to measure bound protein and is reported as a percentage of wild-type binding from each experiment, normalized for KRIT1 loading. Error bars indicate the standard error of the mean (S.E.M.) for three independent experiments. (**C**) WT indicates wild-type KRIT1; NY/AA, N192A^{KRIT}/Y195A^{KRIT} (to impact *NPxY* site binding); RR/AA, R179A^{KRIT}/R185A^{KRIT} (to impact *RR* site binding) and AP/DD, A176D^{KRIT}/P182D^{KRIT} (to impact *RR* site binding). (**D**) WT indicates wild-type ICAP1; LII/AAA, L135A^{ICAP}/I138A^{ICAP}/I139A^{ICAP}; C184D, C184D^{ICAP}; I89R, I89R^{ICAP}; DQ/AA, D93A^{ICAP}/Q96A^{ICAP}. See also Figure S2.

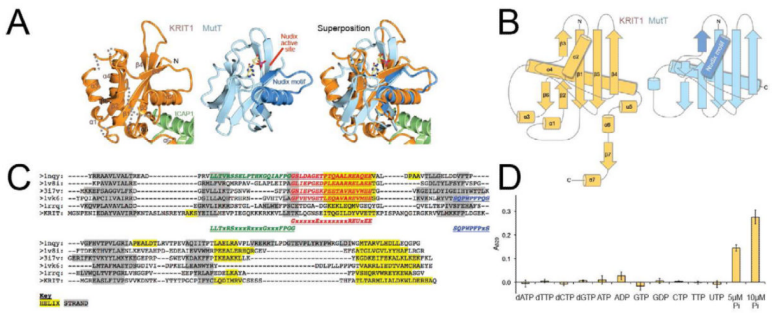

Fig. 3. KRIT1 contains an N-terminal Nudix domain

A) Comparison and superposition of the KRIT1 Nudix domain with the crystal structure of MutT hydrolase in complex with 8-OXO-dGMP (PDB ID: 3A6U)(Nakamura et al., 2010). The locations of the Nudix motif and active site in MutT are indicated. The bound nucleotide is shown in stick format. The superposition shows that KRIT1 N-terminal domain folds as a Nudix domain, similar to the founder member of the family, MutT. **B)** Topology maps of the KRIT1 and MutT Nudix domains. α-helices shown as cylinders and β-strands as arrows. The Nudix motif of MutT is indicated. **C)** Structure-based sequence alignment of KRIT1 Nudix domain with the Nudix domains of five representative members of the domain family. The structures aligned with KRIT1 are: 1nqy, a CoA pyrophosphatase from *D. Radiodurans*; 1v8i, an ADP-ribose pyrophosphatase; 3i7v, an AP4A hydrolase from *Aquifex eolicus*; 1vk6, an NADH pyrophosphatase from *E. Coli* (unpublished); and 1rrq, a MUTY adenine glycosylase. β-strands are shaded grey, and α-helices shaded yellow. The "Nudix box" motif (**GxxxxxExxxxxxxREUxEExGU**) is shaded red and highlighted where present. The CoA enzyme (**LLTxRSxxxRxxxGxxxFPGG**) and NADH diphosphatase hydrolase (**SQPWPFPxS**) motifs are also indicated where present. KRIT1 does not contain any of the conserved motifs. **D)** Hydrolase assay for KRIT1 Nudix domain. 50 μM (d)NTPs were incubated with 1 μM purified KRIT1-ICAP1 in the presence of $MgCl_2$ and the reaction analyzed using Malachite green reagents. Controls of 5 μM and 10 μM phosphate standard were included. The assay shows no hydrolase activity for the KRIT1 Nudix domain against this panel of known Nudix hydrolase substrates. Results are mean ± S.E.M. for 4 independent experiments. See also Figure S4.

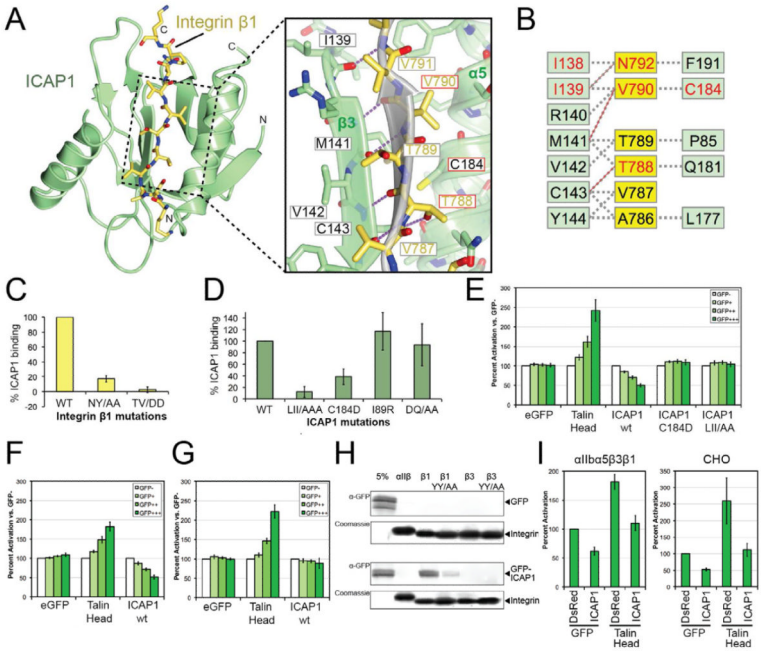

Fig. 4. Structural basis for ICAP1 repression of integrin β1 activation

A) Co-crystal structure of ICAP1 in complex with integrin β1; ICAP1 (green), integrin β1 (yellow). Exploded view shows that integrin β1 forms a β-sheet extension from ICAP1 strand β3. Residues mutated in this study are boxed in red. **B)** Schematic map showing the interactions between integrin β1 (yellow) and ICAP1 (green). Mutated residues are colored red. Hydrogen bonds indicated by red lines, and non-bonding contacts as dashed lines. **C,D)** Validation of the binding interface by mutagenesis. Binding of wild-type and mutant ICAP1$^{49–200}$ to wild-type or mutant β1$^{752–798}$ was assessed by pull-down, quantified by densitometry and is reported as mean percentage of wild-type binding ± SEM for three independent experiments. WT indicates wild-type, NY/AA, N792A^{Iβ1}/Y795A^{Iβ1}; TV/DD, T788D^{Iβ1}/V790D^{Iβ1}; LII/AAA, L135A^{ICAP}/I138A^{ICAP}/I139A^{ICAP}; C184D, C184D^{ICAP}; I89R, I89R^{ICAP}; DQ/AA, D93A^{ICAP}/Q96A^{ICAP}. For ICAP1 mutations in the *RR* site (I89R, DQ/AA) there is no detectable alteration in binding. **E–G)** ICAP1 binding to the integrin β tails is required to suppress integrin activation CHO cells were transfected with GFP, GFP-ICAP1$^{49–200}$, or GFP-ICAP1$^{49–200}$ mutants and the activation of stably expressed chimeric αIIbα5β3β1 integrins (**E**), αIIbβ3 (**G**) or endogenous α5β1 integrins (**F**) was assessed by flow cytometry. Gating on cell populations with different GFP intensities permits analysis of the dose-dependency of effects. Talin head activates all integrins in this assay. Results are the mean percentage ± S.E.M of the untransfected (GFP-) population from at least 3 independent experiments. **H)** Western blot pull-down showing GFP-ICAP1$^{49–200}$ binds better to recombinant integrin β1 tails than β3 tails. **I)** Integrin activation assay showing that ICAP1 suppresses talin head-mediated activation of β1 integrins. CHO cells stably expressing chimeric αIIbα5β3β1 integrins (left panel) or wild-type CHO cells (right panel) were co-transfected with GFP or GFP-talin head and DsRed or DsRed-ICAP1$^{49–200}$ and activation assessed using PAC1 or FN9-11 as appropriate. Results are the mean percentage ± S.E.M of the GFP+DsRed control from at least 3 independent experiments. See also Figure S5.

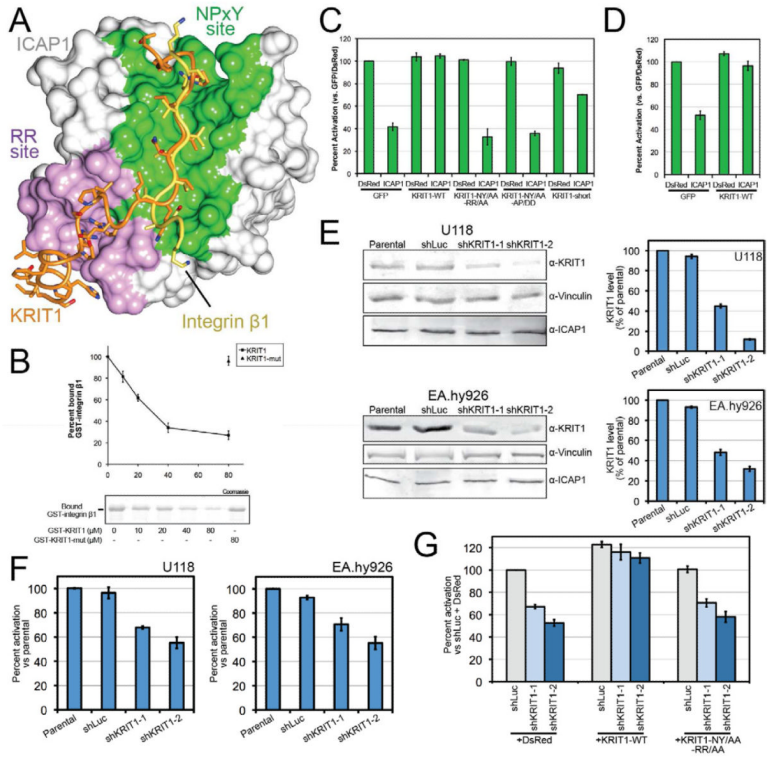

Fig. 5. The KRIT1-ICAP1 axis of integrin regulation

A) Superposition of the integrin β1-ICAP1 and KRIT1-ICAP1 crystal structures with the surface of ICAP1 shown. Integrin β1 (in yellow) and KRIT1 (in salmon) directly compete to bind the "*NPxY*" site of ICAP1 shown in green, however, only KRIT1 binds the "*RR*" site shown in purple. **B)** Competition assay. Increasing amounts of GST-KRIT1 (170–198) competes with GST-integrin β1 to bind ICAP1 immobilized on nickel beads, however GST-KRIT1-mut (quadruple mutation A176D^{KRIT}/P182D^{KRIT}/N192A^{KRIT}/Y195A^{KRIT}) displays significantly reduced competition. This shows that integrin β1 and KRIT1 compete to bind ICAP1. Error bars indicate S.E.M. for 3 independent experiments. **C** and **D)** Integrin activation assays in CHO cells show that co-expression of GFP-KRIT1$^{1–198}$ with DsRed-ICAP1$^{49–200}$ rescues ICAP1 suppression of activation of chimeric αIIbα5β3β1 integrins (**C**) or endogenous CHO cell α5β1 (**D**) and that quadruple KRIT1 mutations NY/AA-RR/AA (R179A^{KRIT}/R185A^{KRIT}/N192A^{KRIT}/Y195A^{KRIT} and NY/AA-AP/AA (A176D^{KRIT}/P182D^{KRIT}/N192A^{KRIT}/Y195A^{KRIT}) prevent rescue. A short KRIT1 construct (residues 170–198, KRIT1-short) is less effective at rescue of ICAP1 suppression of integrin activation. Error bars indicate S.E.M. for at least 3 independent experiments. **E)** Quantification KRIT1 knock-down. Lysates from shRNA infected U118 and EA.hy926 cells were detected in an anti-KRIT1 immuno-blot and bands were quantified using ImageJ. Bar graph shows the average of three separate blots +/− S.E.M. **F)** Integrin activation assays in U118 and EA.hy926 cells show that activation of endogenous α5β1 is suppressed upon KRIT1 knockdown. Error bars indicate S.E.M. for 4 independent experiments. **G)** The suppression of α5β1 activation in KRIT1-knockdown cells is reversed when wild-type DsRed-KRIT1$^{1–198}$ is expressed but quadruple KRIT1 mutation NY/AA-RR/AA (R179A^{KRIT}/R185A^{KRIT}/N192A^{KRIT}/Y195A^{KRIT}) prevents rescue. Error bars indicate S.E.M. for 3 independent experiments. See also Figure S6.

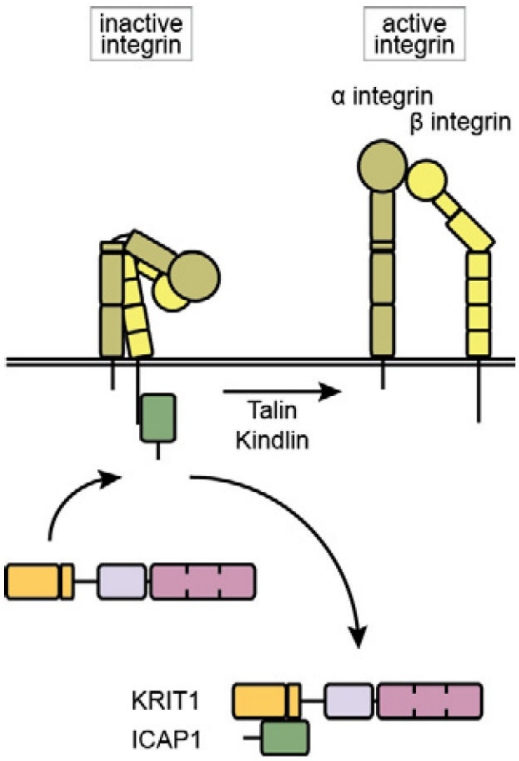

Fig. 6. Schematic of the KRIT1-ICAP1 switch for integrin activation

ICAP1-binds integrin β1 cytoplasmic tail and protects from talin- or kindlin-mediated activation. Activated KRIT1 is recruited to ICAP1 by the *RR* site and displaces integrin by the *NPxY* site. This sequesters ICAP1 from integrin to allow talin- and kindlin-mediated integrin activation.